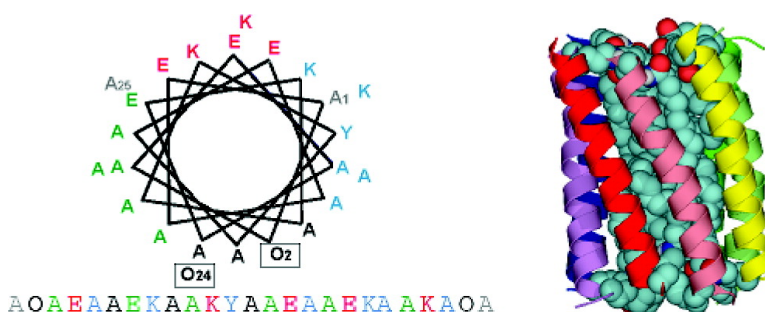


Molecular Models of Lipopeptide Detergents: Large Coiled-Coils with Hydrocarbon Interiors

Evan Kelly, Gilbert G. Priv, and D. Peter Tieleman

J. Am. Chem. Soc., **2005**, 127 (39), 13446-13447 • DOI: 10.1021/ja051275n • Publication Date (Web): 09 September 2005

Downloaded from <http://pubs.acs.org> on March 25, 2009



More About This Article

Additional resources and features associated with this article are available within the HTML version:

- Supporting Information
- Access to high resolution figures
- Links to articles and content related to this article
- Copyright permission to reproduce figures and/or text from this article

[View the Full Text HTML](#)

Molecular Models of Lipopeptide Detergents: Large Coiled-Coils with Hydrocarbon Interiors

Evan Kelly,[†] Gilbert G. Privé,[‡] and D. Peter Tieleman*[†]

Department of Biological Sciences, Structural Biology Research Group, University of Calgary, 2500 University Drive NW, Calgary, Alberta, Canada T2N 1N4, and Department of Medical Biophysics and Department of Biochemistry, University of Toronto, Ontario Cancer Institute, 610 University Avenue, Toronto, Ontario, Canada M5G 2M9

Received March 1, 2005; E-mail: tieleman@ucalgary.ca

The crystallization of a membrane protein typically requires a solubilized sample that is stabilized in a gentle, nondenaturing detergent.¹ Detergents that form small micelles often favor membrane protein crystallization, but these also have the highest tendency to disrupt a protein's native structure. Recently, a new class of detergents, named lipopeptide detergents (LPDs), was introduced that consists of designed α -helical peptides with attached acyl chains.² These detergents have the ability to preserve protein structure while forming relatively small protein–detergent complexes. Here, we describe molecular models of micelles formed by these novel amphiphiles. The models explain the observed stability and aggregation behavior of LPDs with different alkyl chain lengths. They show a novel coiled-coil structure of the peptide assemblies and a strongly ordered hydrocarbon interior and suggest new ways to further diversify these detergents.

The LPDs studied are peptides with the sequence acetyl-AOAEAAEKAAYAAEAAEKAOKAOA-amide. The “O” residues are ornithines to which acyl chains with variable lengths are attached. Thus, LPD12, LPD16, and LPD20 are peptides which each contain two acyl chains of length 12, 16, or 20, respectively. The detergents are designed to form amphipathic α -helices such that the alkyl chains associate with the alanine-rich face of the peptides. Equilibrium centrifugation has shown that LPD12 and LPD16 self-associate into octameric complexes, while lipopeptides with longer chains form larger, less well-defined complexes.²

We used molecular dynamics simulations to investigate the properties and dynamics of LPD12, LPD16, and LPD20 micelles. Detailed methods are available as Supporting Information. We constructed micelles with parallel and antiparallel helices using a simulated annealing/restrained molecular dynamics (SA/MD) protocol³ as well as using idealized geometries. After clustering of the SA/MD results, we selected top-ranking structures for MD simulations in explicit solvent and salt solution mimicking the experimental conditions.² The main octameric models are designated P12 (parallel, C12 chains), A12, A16, and A20 (all three antiparallel), respectively (Table S1).

In all simulations, the α -helices formed a cylindrical shell surrounding the acyl chains. The acyl chains were largely contained within the inside of the micelle. Root mean square deviations (RMSD) from the starting models increase rapidly to about 0.2 nm and level off after several nanoseconds at values of 0.3–0.4 nm (Figure S1). The simulation starting from an idealized antiparallel geometry rapidly reaches the highest RMSD of all the simulations. The secondary structure remains mostly stable over the length of the simulations, with only some reversible fraying at the ends of the helices (details not shown). The radius of gyration of each

micelle stabilizes by about the 3 ns mark, except for A20, which continues to fluctuate (Figure S2). The A12 and P12 micelles have the same size, while A16 is slightly larger, and A20 is the largest, consistent with the observed solution light scattering data.² We also estimated the hydrodynamic radius, which takes into account a layer of boundary water around the micelle. The results are generally the same as that for the radius of gyration, but the radii obtained are approximately 0.5 nm larger for all simulations. The α -helices in the P12, A12, and A16 simulations pack side-by-side with neighboring helices, sequestering the acyl chains in the inside of the assemblies. The A20 simulation, in contrast, reveals a “tear” in the lateral packing of two of the LPD monomers. In A16, an acyl chain occasionally escapes the micelle interior, only to reinsert later. In all cases, small hydrophobic surfaces remain exposed at the ends of the cylindrical micelles. The overall fraction of hydrophobic exposed area is similar for A12, P12, and A16 (ca. 0.60 on average), but larger for A20 and still increasing after 20 ns (0.63 at 20 ns) (Figure S3). Combined, these properties suggest A20 is not a stable octamer, consistent with experimental measurements of a larger aggregation state.² Simulations with hexameric micelles reveal tears in the peptide surface, exposing lipid to the solvent. This suggests the LPD hexamers are too small to effectively bury the coupled acyl chains. In contrast, decameric micelles deform because the interior volume of the helical bundle is larger than that of the associated chains (Figure S4).

There are 18 possible combinations of helix orientations in an octameric complex, but it is difficult to address which one is most favorable. We only modeled the all-parallel and all-antiparallel cases. In the latter, helices alternate in orientation. Although we cannot calculate a reliable free energy difference between two micelles, A12(I) and P12(II) have exactly the same composition and we can compare their total potential energies averaged over the final 5 ns. A12(I) has a lower average energy by 326 kJ for the whole system, but the standard deviation in the total potential energy in each simulation is ca. 500 kJ/mol. Our best statistical estimate of the error in the difference is 14 kJ/mol (see methods in the Supporting Information), suggesting the antiparallel orientation is preferred. The factors that may affect the preferred helix orientation include the macrodipole moment of the helices (which would favor an antiparallel orientation), inter-helix packing, and ionic side chain interactions.

The strongly confining cylindrical interior is an unusual feature of the lipopeptide micelles, with interesting consequences for the acyl chains (Figure 1). As a consequence of the linkage to the peptide scaffolding, the first dihedral angles in the acyl chains are relatively constrained and have trans fractions in the range of 0.8 to 0.85, as compared to 0.65 for liquid decane at the same temperature.⁴ For the angles 2–7, the acyl chain values drop to

[†] University of Calgary.

[‡] University of Toronto.

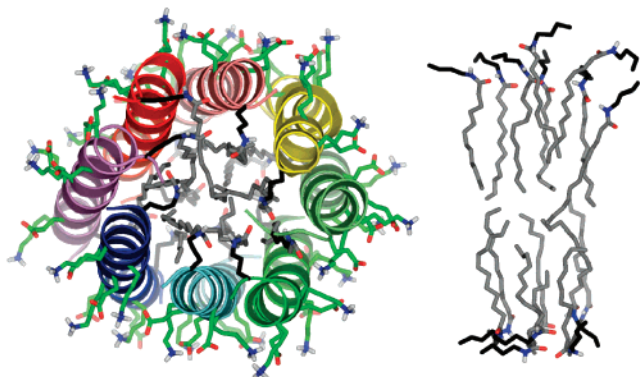


Figure 1. Representation of the final structure of A12(II). *Left:* End-on view of the cylindrical assembly. The ornithines are drawn as sticks with black carbon atoms and are coupled via amide bonds to C12 alkyl chains in gray. The lysine and glutamates face the exterior and are shown in stick representation with green carbons. *Right:* Side view of the 16 acylated ornithines.

0.75–0.80, while this value rises to about 0.7 in the free alkanes. By the end of the chains, the LPD acyl values range from 0.65 to 0.7, which is very near those of the free decane and dodecane at 0.65 (Figure S5). The average rotation time for the LPD chains, however, was approximately 4000 ps, which is much larger than ca. 25 ps for liquid alkanes at the same temperature.⁴ Thus, lipopeptide micelles provide a unique environment for acyl chains, with significantly more ordered chains and very slow chain dynamics reminiscent of the slow dynamics in lipid gel phases.⁵

The individual helices have typical α -helical parameters when compared to several experimentally determined coiled-coil structures of different sizes (Table S2), with the exception of slightly shorter helix–helix separations. The pairwise crossing angles are shallower than typical values from natural helix–helix interactions. Analysis of the helix geometries with the TWISTER algorithm clearly showed coiled-coil geometries for most octameric bundles and identified residues that face the supercoil axis.^{6a} The 25-residue sequence contains two stutters that change the register of the otherwise regular consensus heptad repeat assignments determined over the last 5 ns of each trajectory. TWISTER is nevertheless able to assign the two ornithine residues and four of the alanines to inward-facing *a* and *d* positions. The three glutamates and four lysines are all assigned to the hydrophilic *b*, *c*, and *f* positions. The helix crossing angle values ranged from +15 to +10° in the A12 and A16 models. A20 and P12 had a lesser degree of supercoiling with crossing angles of 3–4° for A20, indicating nearly straight helices, and –7° in P12, indicating right-handed supercoiling. Detailed values are given in Figure S6. The P12(IDEAL) simulation is the only one with a negative crossing angle through the entire 10 ns simulation. The coiled-coil radius and pitch are strongly dependent on the number of constituent strands⁶ (Table S2). In addition, the radii are larger for A16 and A20 relative to that of A12 since these micelles have to accommodate larger amounts of hydrocarbon, despite having identical amino acid compositions and the same number of helices. A comparison of A12, A16, and A20 indicates that the main adjustments are in the coiled-coil radius, which is coupled to the superhelical pitch and to the helix crossing angles. In addition, there is a distinct barrelling effect. The diameter of the assembly in the middle of the bundles is larger by up to 1 Å compared to the ends of the bundle, through a slight bending of the helices.

This plasticity may be a result of the alanine-rich character of the peptide–peptide interfaces (Figure S7). Four distinct environments occur along the length of each α -helix; there are two distinct helix–helix neighbor packing contacts in addition to the surface buried in the lipidic core and the solvent-exposed hydrophilic face (Figures 1 and S7). Each peptide buries ~ 250 Å² in the lipidic core and has a contact area of approximately 400 Å² with each of the two neighboring helices, leaving an area of ~ 1200 Å² per peptide exposed to the bulk solvent. Since there are no large hydrophobic residues in the peptides, the alanine surfaces are relatively featureless and the helix crossing angles are not as constrained by the packing motifs that are seen with more complex natural sequences. Accordingly, an analysis of local interactions with the SOCKET method⁷ finds only very limited local knobs-into-holes packing. This feature is also likely to be important in the formation of a LPD complex with an integral membrane protein since the LPD–LPD interactions must adjust in order to accommodate different-sized guests. Further structural studies on LPD–guest complexes will provide additional insight into these interactions.

Together, the simulations suggest that the stability of the aggregates is driven more by the burial of the acyl chains than by peptide–peptide contacts. This is in agreement with the result that a nonacylated LPD control peptide is monomeric and unstructured in solution.² A control simulation in which the lipid chains were removed from a stable octamer shows major destabilization on a 10 ns time scale. In the octameric LPD12 and LPD16 simulations, the overall bundle structure is maintained in 10 ns simulations, while LPD20 shows significant defects that would make the micelle unstable, consistent with the experimentally observed capacity of 12–16 carbons per chain within an octamer. The chains themselves have a very rigid and ordered geometry, comparable to that of crystalline lipids, and both parallel and antiparallel helices can pack with compelling geometry. These insights provide a framework for continuing the development of the LPD design for specific applications, including membrane protein crystallization.

Acknowledgment. D.P.T. is an AHFMR Senior Scholar. E.K. was supported by an AHFMR summer studentship. This work was supported by CIHR (G.G.P. and D.P.T.) and WestGrid. We thank Walter Ash for his help with the implementation of TWISTER.

Supporting Information Available: Detailed methods and simulation results (Tables S1 and S2, Figures S1–S7) in PDF format. This material is available free of charge via the Internet at <http://pubs.acs.org>.

References

- (a) Wiener, M. C. *Methods* **2004**, *34*, 364–372. (b) Seddon, A. M.; Curnow, P.; Booth, P. J. *Biochim. Biophys. Acta* **2004**, *1666*, 105–117. (c) Nollert, P. *Prog. Biophys. Mol. Biol.* **2005**, *88*, 339–357. (d) Schafmeister, C. E.; Miercke, L. J. W.; Stroud, R. M. *Science* **1993**, *262*, 734–738. (e) Bayburt, T. H.; Sligar, S. G. *Protein Sci.* **2003**, *12*, 2476–2481.
- McGregor, C. L.; Chen, L.; Pomroy, N. C.; Hwang, P.; Go, S.; Chakrabarty, A.; Privé, G. *Nat. Biotechnol.* **2003**, *21*, 171–176.
- (a) Nilges, M.; Brunger, A. T. *Proteins* **1993**, *15*, 133–146. (b) Ash, W. L.; Stockner, T.; MacCallum, J. L.; Tieleman, D. P. *Biochemistry* **2004**, *43*, 9050–9060.
- Tieleman, D. P.; van der Spoel, D.; Berendsen, H. J. C. *J. Phys. Chem. B* **2000**, *104*, 6380–6388.
- Mayer, C.; Muller, K.; Weisz, K.; Kothe, G. *Liq. Cryst.* **1988**, *3*, 797–806.
- (a) Strelkov, S. V.; Burkhard, P. *J. Struct. Biol.* **2002**, *137*, 54–64. (b) Walshaw, J.; Woolfson, D. N. *J. Struct. Biol.* **2003**, *144*, 349–361. (c) Calladine, C. R.; Sharff, A.; Luisi, B. *J. Mol. Biol.* **2001**, *305*, 603–618.
- Walshaw, J.; Woolfson, D. N. *J. Mol. Biol.* **2001**, *307*, 1427–1450.

JA051275N